ACS Catalysis

pubs.acs.org/acscatalysis

Research Article

Direct Conversion of Renewable CO_2-Rich Syngas to High-Octane Hydrocarbons in a Single Reactor

Claire T. Nimlos, Connor P. Nash, Daniel P. Dupuis, Anh T. To, Anurag Kumar, Jesse E. Hensley, and Daniel A. Ruddy*

Cite This: *ACS Catal.* 2022, 12, 9270−9280

Read Online

ACCESS | Metrics & More | Article Recommendations | Supporting Information

ABSTRACT: The synthesis of branched hydrocarbons for high-octane gasoline and sustainable aviation fuel directly from CO_2-rich syngas in a single reactor holds potential to decrease capital and operating costs and increase overall energy and carbon efficiencies in a biorefinery. Here, we report the cascade chemistry of syngas to hydrocarbons under mild reaction conditions in a single reactor with C_{4+} single-pass yields of 13.7−44.9%, depending on the relative catalyst composition employing our dimethyl ether homologation catalyst, Cu/BEA zeolite. With co-fed CO_2 at a concentration representative of biomass-derived syngas, 2.5:1:0.9 for H_2:CO:CO_2, a hydrocarbon yield of 12.2% was observed with similar selectivity to C_{4+} products compared to the CO_2-free feed. Definitive evidence of CO_2 incorporation into the hydrocarbon products was demonstrated with isotopically labeled $^{13}CO_2$ co-feed experiments, where mass spectrometry confirmed the propagation of ^{13}C into the C_{4+} hydrocarbons, highlighting the feasibility to co-convert CO and CO_2 in this single reactor approach.

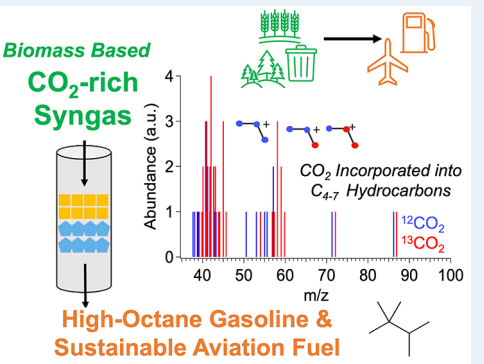

KEYWORDS: *syngas to hydrocarbons, cu/BEA zeolite, biomass syngas, high-octane gasoline, sustainable aviation fuel, CO_2 conversion*

1. INTRODUCTION

A variety of carbon sources, including renewable sources, can be converted to synthesis gas (syngas), a mixture of carbon monoxide (CO) and hydrogen (H_2), through well-established gasification processes.[1−3] Syngas is converted to hydrocarbons (HCs) through "gas-to-liquid" methods, such as Fischer−Tropsch synthesis, or via intermediates such as methanol (MeOH) or dimethyl ether (DME). The methanol-to-gasoline (MTG) process is one example of a technologically mature process based on syngas-derived MeOH. The conventional MTG process yields gasoline-range HCs with a high concentration of aromatics to provide appropriate octane rating, but aromatic content in gasoline is limited by current fuel standards.[4] The high pressure and temperature conditions (340−510 °C, 2 MPa) required for the MTG process combined with low per-pass yields results in high capital and operating costs, especially at smaller scales typical of biorefineries.[5] Conversely, a recently developed process termed the "High-Octane Gasoline (HOG) pathway" converts MeOH/DME intermediates to branched C_{4-7} species over beta zeolite (BEA) catalysts, operates at lower temperatures and pressures (175−225 °C, 0.1−0.3 MPa), and produces a high-octane, high-value gasoline product without aromatics.[6−8] The HOG product lacks an inherent blend limit, and it is especially rich in branched species, such as 2,2,3-trimethylbutane (triptane), which has a research octane number of 112.8.[9] Catalyst development from our group has demonstrated that a multifunctional Cu-modified beta zeolite catalyst (Cu/BEA) converts DME with co-fed H_2 to the HOG product with improved per-pass yield, lifetime, and regenerability compared to previously reported Brønsted acid zeolites.[10−12] In recent work, we also assessed the viability of a biorefinery concept centered around the HOG pathway, where process models and techno-economic analysis (TEA) demonstrated a 38% overall yield increase afforded by Cu/BEA through recycle and reincorporation of the C_4 products.[5,11] Furthermore, this biorefinery concept highlighted the versatility of the C_{4+} products to provide an attractive route to sustainable aviation fuel (SAF) via known and relatively inexpensive downstream processing.[11]

Recently, several reports focused on process intensification for the direct conversion of syngas-to-hydrocarbons (STH) through MeOH and DME intermediates in a single step.[1,13] A single-step process holds the potential to decrease capital and operating costs and increase the overall energy efficiency. However, envisioning a bifunctional catalyst or multicomponent catalyst to directly convert syngas via a MeOH/DME

Received: May 2, 2022
Revised: July 6, 2022
Published: July 15, 2022

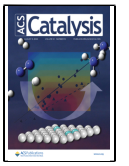

intermediate presents a formidable challenge due to mismatched process conditions, especially reaction temperature: lower temperatures (200−250 °C) are commonly employed for MeOH synthesis, but higher temperatures (>350 °C) are typically utilized for methanol-to-hydrocarbons (MTH) reactions (Figure 1).[1,14,15] Early studies utilized multi-component catalysts, such as mixtures of Cu/ZnO or $PdSiO_2$ with USY zeolite, to act as MeOH synthesis and HC synthesis catalysts, respectively. These reports observed up to 77% HC selectivity to C_{3-4} paraffin products under intermediate reaction temperatures (≤325 °C) and pressure (2.1 MPa).[16,17] In more recently reported cases, this temperature mismatch was addressed by developing high-temperature MeOH or alcohol synthesis catalysts combined with high-temperature HC synthesis catalysts. Metal oxides (e.g., $Zn_2Mn_1O_x$) combined with large-pore zeolites, commonly denoted "OX-ZEO" (Oxide-Zeolite), offer a high temperature and pressure (360 °C, 4 MPa) STH route, exploiting a controlled C−C coupling concept to form gasoline-range products with high C_{5-11} selectivities (63−76%).[18,19] For OX-ZEO systems, aromatic formation increased with higher-dimension zeolite pores (1D to 3D) because of the larger intersection voids.[18] Dagle et al. demonstrated that physical mixtures of Pd-based MeOH synthesis catalyst (e.g., $Pd/ZnO/Al_2O_3$) with ZSM-5 (MFI zeolite) converted syngas to aromatic-rich gasoline-range (C_{5+}) HCs at high temperatures and pressures (310−375 °C, 2−6 MPa).[20] In this system, higher selectivity to larger carbon products (C_{6+} branched and cyclic species) was observed at lower temperatures (310 °C vs 370 °C) or with increasing zeolite pore size (FAU vs MFI topology). Furthermore, it was demonstrated that 0.5 wt % Pd on a FeCoCu support mixed with the ZSM-5 catalyst decreased the undesired durene formation.[21] Another approach for direct syngas-to-olefins utilized multicomponent $ZnO\text{-}ZrO_2/SAPO\text{-}34$ catalysts at high temperatures and pressures (400 °C, 1−4 MPa). Control of the Zn/Zr ratio and increasing the proximity of the metal oxide to the zeolite pores (millimeter to nanoscale distances) increased CO conversion and olefin selectivity until a maximum was reached at ca. 29% CO conversion with a C_{2-4} olefin selectivity of 77%.[22,23] Rather than a single bed to effect the STH reaction, recent work by Ni, et al. employed a dual-bed reactor at intermediate temperature and high pressure (260−320 °C and 3 MPa), utilizing commercial catalysts for MeOH and DME synthesis ($CuZnO/Al_2O_3$ and $\gamma\text{-}Al_2O_3$ respectively) upstream of a reactor with a nanosized ZSM-5 catalyst for HC synthesis. This reactor system effectively converted syngas to C_{5-11} HCs for 110 h.[13] These reports of single-step cascade reactions to achieve direct STH, which occur under conditions enabling both syngas-to-methanol and MTH chemistries, provide conceptual improvements in process chemistry compared to multi-step processes.[14,15]

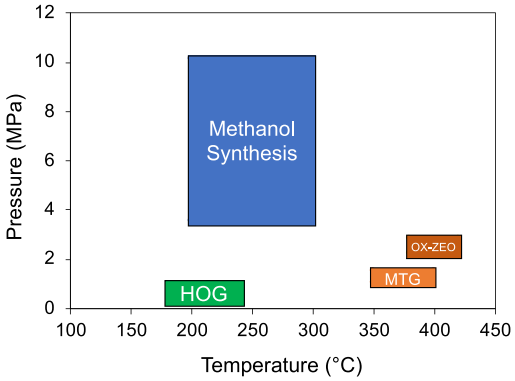

Figure 1. Pressure and temperature conditions typically employed for MeOH synthesis, the HOG pathway, MTG, and OX-ZEO.[1,3,14]

Connecting the catalyst and process design concepts from these previous reports with our recent development of the HOG pathway, we recognized the opportunity to eliminate the mismatched reaction conditions noted above, while generating a high-quality product. This is especially evident for reaction temperature, where HOG synthesis occurs in the same range as MeOH synthesis (Figure 1). This temperature overlap enables the use of the relatively inexpensive and commercial $CuZnO/Al_2O_3$ MeOH synthesis catalyst, avoiding the need to develop a new MeOH synthesis catalyst or use precious metals, such as Pd. Furthermore, MeOH dehydration to DME occurs under these conditions over inexpensive and commercial acid catalysts, such as $\gamma\text{-}Al_2O_3$. Our previous reports focused on HOG synthesis at low pressures (i.e., below 0.5 MPa), but the knowledge that MTH chemistry proceeds at higher pressures over many zeolite catalysts led us to hypothesize that a moderate pressure of 0.5−1.5 MPa could be employed with H/BEA and Cu/BEA catalysts, while utilizing commercial MeOH/DME synthesis catalysts at lower pressures than commonly employed.

CO_2 is a byproduct of gasification, and it is commonly removed from the process (or reduced to a target value, such as 5% CO_2 in syngas for MeOH synthesis) during a clean-up step prior to downstream conversion. Biomass-derived syngas contains a high concentration of CO_2, ranging from 19−23% of reformed syngas,[24] and therefore, utilization of this carbon source would provide an avenue to substantially improve carbon efficiency and overall fuel product yield in a syngas conversion process. Furthermore, CO_2 is known to form under STH process conditions through the water-gas shift reaction over metallic Cu sites[25,26] and as an intermediate during the conversion of syngas to methanol on CZA.[27,28] In addition to the process intensification approach to gain operational efficiencies by using a single reactor, carbon-efficiency gains in the STH reaction network may be achieved via co-conversion of CO_2 in the STH reaction network.

Here, we report a single reactor approach to convert syngas to branched hydrocarbon products, where commercially available MeOH synthesis and MeOH dehydration catalysts are combined with H/BEA and Cu/BEA HC synthesis catalysts. Single-pass CO conversions up to 77% with corresponding C_{4+} carbon yields up to 44.9% were observed under the conditions employed here. Furthermore, we demonstrated that carbon from CO_2 co-fed with syngas was incorporated into HC products with similar HC selectivity (i.e., low methane and high C_{4-7} selectivity), evidenced by the incorporation of ^{13}C into C_{4+} products in isotopically labeled $^{13}CO_2$ co-feed experiments. This STH process intensification approach using a single reactor provides a new avenue to improve operational efficiency and carbon efficiency in the HOG pathway, highlighted by high per-pass C_{4+} yields, and importantly, incorporation of CO_2-derived carbon into the hydrocarbon products.

https://doi.org/10.1021/acscatal.2c02155
ACS Catal. 2022, 12, 9270−9280

2. EXPERIMENTAL SECTION

2.1. Catalyst Preparation. Commercial BEA zeolite in the NH_4^+ form (Tosoh, SiO_2/Al_2O_3 = 27, Si/Al = 13.5; 45−125 μm particle sizes) was heated to 550 °C at 2 °C min^{-1} in flowing zero air for 8 h to produce the proton form, denoted H/BEA. To produce a nominally 5 wt % Cu/BEA catalyst, an aqueous solution of $Cu(NO_3)_2{\cdot}2.5\ H_2O$ was added dropwise to powdered NH_4-BEA until the incipient wetness point was achieved, as previously reported.[10,11] The slurry was then mixed and dried at 50 °C in flowing air overnight, followed by oxidative treatment to 500 °C at 2 °C min^{-1} in flowing zero air for 6 h. Elemental analysis determined a Cu loading of 4.75 wt %. Additional catalyst materials used for MeOH synthesis ($CuZnO/Al_2O_3$, "CZA", Clariant, MegaMax 800) and DME synthesis (γ-Al_2O_3, "A", Saint-Gobain NorPro, SA6173) were acquired from commercial sources.

2.2. Catalyst Characterization. The Cu content was determined by elemental analysis performed by Galbraith Laboratories Inc. (Knoxville, TN) using inductively coupled plasma optical emission spectroscopy. Powder X-ray diffraction (PXRD) patterns were collected using a Rigaku Ultima IV diffractometer operated at 40 kV and 44 mA with a Cu Kα X-ray source. Diffraction patterns were measured in the 2θ range of 4°−60° to confirm the BEA structure after addition of Cu, and the data matched those previously reported.[10] Extensive characterization of the metallic and ionic nature of the Cu species present in Cu/BEA has been previously reported.[10]

Brønsted acid site density was quantified using temperature-programed desorption of isopropylamine (IPA-TPD) for the Cu/BEA and H/BEA materials, as previously reported.[9] Catalyst samples (ca. 200 mg) were sieved to 212−300 μm size and pretreated in 150 $cm^3\ min^{-1}$ of 95% H_2/5% Ar to 300 °C at 2 °C min^{-1} ramp and held for 2 h. The sample was then cooled to 100 °C and purged with inert gas (95% N_2/5% He). When the bed temperature stabilized at 100 °C, 1 mL of IPA was introduced slowly via a syringe over 10 min to saturate the sample. The sample was then purged in inert flow (95% N_2/5% He) for at least 12 h at 100 °C to remove physiosorbed IPA. The TPD was performed with a 10 °C min^{-1} ramp to 500 °C, and a Pfeiffer PrismaPlus mass spectrometer monitored the desorbed products, with the propylene signal used to quantify H^+ site density. The propylene signal (m/z = 41) was calibrated with 5 mL propylene pulses and normalized to the internal standard He signal (m/z = 4). The Brønsted acid site densities for H/BEA and Cu/BEA were determined to be 805 and 925 mmol/g, respectively.

2.3. Syngas to Hydrocarbon Reaction Testing. CZA and A catalysts were crushed in a porcelain mortar and pestle and sieved to 212−300 μm size. Cu/BEA powders were pressed (22 kN), crushed in a porcelain mortar and pestle, and sieved to 212−300 μm size. Approximately 1.10 g of CZA, 0.35 g of A, and 0.35−1.10 g of Cu/BEA (or H/BEA) were loaded into the reactor depending on the composition tested. To create a "mixed-bed" configuration, catalysts were physically mixed, then diluted with 177−250 μm low surface-area silicon carbide (SiC) to achieve the same bed volume (4.2 ± 0.2 cm^3) for each run and to minimize channeling, axial dispersion, and temperature gradients in the bed. The "stacked-bed" configuration was achieved by loading two beds, each physically mixed with SiC, separated by a plug of quartz wool. Here, notation for a mixed bed uses the "+" symbol, (e.g., catalyst1 + catalyst2 + catalyst3), and stacked-bed configuration is denoted using a vertical bar symbol "|", (e.g., catalyst1|catalyst2). Specifically, a combination of mixed and stacked catalysts was employed in our typical stacked-bed configuration, leading to both + and | notation, such as CZA +A|H/BEA, whereby CZA and A are physically mixed and located upstream of H/BEA. The catalysts were loaded into a 7.9 mm ID stainless-steel tubular reactor placed within an electric furnace operating in downflow configuration with a four-point thermocouple to monitor reaction temperature (typical variation in a temperature of ±0.25 °C). Catalyst beds were loaded into the reactor and positioned within the isothermal zone using quartz chips and quartz wool. Mass flow controllers (Brooks Instrument) were used to control gas flow rates to the reactor and were calibrated for the specific gas streams prior to use.

Prior to the STH reaction, the catalyst bed was reduced with 25 $cm^3\ min^{-1}$ of H_2, ramped at 1.0 °C min^{-1} to 180 °C then at 0.5 °C min^{-1} to 230 °C, and held for 2 h before cooling to the reaction temperature of 220 °C. The reactor was pressurized to 750 kPa absolute and was maintained using a Badger Meter research control valve. The pressure at the reactor inlet and effluent were monitored, and pressure drop across the catalyst bed was negligible (<15 kPa). A H_2:CO molar ratio of 2:1 (mol_{H2}:mol_{CO}^{-1}) was employed, and the space velocity (SV) of CO relative to the total CZA and A mass loading was controlled at 0.3 or 0.8 $g_{CO}\ g_{CZA+A}^{-1}\ h^{-1}$, where g_{CZA+A} is the combined mass of the CZA and A catalysts. The syngas mixture was prepared in-house using H_2, CO, and Ar to generate a 49:49:2 molar ratio. To achieve H_2:CO ratios of 2 or greater, additional 95% H_2/5% Ar was added using an independent mass flow controller. For CO_2 co-feed experiments, CO_2 was introduced with an independent mass flow controller at a H_2:CO:CO_2 molar ratio of 2.5:1:0.9.

Reactor inlet and outlet gases were sampled through heated (170−200 °C) lines using two Agilent 7890 gas chromatograph (GC) systems. The first GC was equipped with a flame ionization detector (FID) to quantify light hydrocarbons (C_{1-5}) and two thermal conductivity detectors to quantify inert and light permanent gases. The second GC was fitted with two FIDs, one to quantify heavy hydrocarbons (C_{5+}) and the second to quantify oxygenates (MeOH, DME). This second GC was also equipped with an Agilent 5977A mass spectrometry detector (MSD) to measure mass spectra of hydrocarbon products. GC responses for reactants and products (hydrocarbons C_{1-4} and all other products except H_2O) were calibrated using traceable gravimetric gas standards. For hydrocarbons C_5 or higher, GC responses for the respective detector were linearly extrapolated from the FID response of C_{1-4} compounds and confirmed with in-house-prepared C_{5-9} liquid injection standards.

Products and reactants were quantified using Ar as an internal standard and conversion of CO (X_{CO}) was calculated with eq 1:

$$X_{CO} = \frac{\dot{n}_{CO,in} - \dot{n}_{CO,out}}{\dot{n}_{CO,in}} \times 100\% \quad (1)$$

where $\dot{n}_{CO,in}$ and $\dot{n}_{CO,out}$, represent the molar flow rates in (measured by inlets) and out of the reactor of CO ($mol_{CO}\ h^{-1}$), respectively. The product yield for various products, and product groupings (e.g., C_{4+}), was calculated with eq 2:

https://doi.org/10.1021/acscatal.2c02155
ACS Catal. 2022, 12, 9270−9280

$$Y_i = \frac{\dot{n}_{C,i,out}}{\dot{n}_{CO,in}} \times 100\% \quad (2)$$

where $\dot{n}_{CO,in}$ is used as previously defined, and $\dot{n}_{C,i,out}$ is the molar flow rate of carbon in product(s) i. For example, yield to triptane (2,2,3-trimethylbutane) would use $\dot{n}_{C,triptane}$ for $\dot{n}_{C,i,out}$. The product carbon selectivity, S_i (in carbon %, noted as C-selectivity), was calculated via eq 3:

$$S_i = \frac{\dot{n}_{C,i,out}}{\sum \dot{n}_{C,i,out}} \times 100\% \quad (3)$$

where $\dot{n}_{C,i,out}$ is used as previously defined and may be summed over a group of desired products as exemplified for Y_i. The denominator term $\sum \dot{n}_{C,i,out}$ was summed over all products. A corollary to eq 3, carbon selectivity neglecting all oxygenate products (CO_2, MeOH and DME) was calculated via eq 4:

$$S_{i,oxygenate\text{-}free} = \frac{\dot{n}_{C,i,out}}{\sum \dot{n}_{C,i,out} - \sum \dot{n}_{C,oxy,out}} \times 100\% \quad (4)$$

where the $\sum \dot{n}_{C,oxy,out}$ is the sum of carbon molar flow rates of products CO_2, MeOH, and DME. The gravimetric activity of the catalyst, termed productivity, P_i ($g_i\ g_{CuBEA}^{-1}\ h^{-1}$), was calculated with eq 5:

$$P_i = \frac{\dot{n}_i}{m_{CuBEA}} \times M_{Wi} \quad (5)$$

where $\dot{n}_i$ is the molar flow rate of product i ($mol_i\ h^{-1}$), M_{Wi} is the molecular weight of product i ($g_i\ mol^{-1}$), and m_{CuBEA} is the mass of the Cu/BEA catalyst used. Error for selectivities is reported with a 99% confidence interval and is calculated with eq 6:

$$C = Z\frac{\sigma}{\sqrt{n}} \quad (6)$$

where σ is the standard deviation of the data, n is the sample size, and Z is the confidence level value, which is 2.576 for the chosen 99% confidence interval. Cumulative turnover number (TON, eq 7) values are reported in terms of the cumulative mol of carbon in hydrocarbon products per mol of Brønsted acid sites in H/BEA or Cu/BEA at each time point, where t is TOS in h, N_{H+} is the moles of Brønsted acid sites determined by IPA-TPD, and $n_c(t')$ is the total carbon incorporated (mol carbon h^{-1}) in all products except methanol, dimethyl ether, carbon monoxide, and carbon dioxide at time t'.

$$TON(t) = \frac{1}{N_{H+}} \int_0^t dt'\ n_c(t') \quad (7)$$

3. RESULTS AND DISCUSSION

3.1. Approach for STH Using BEA Catalysts. The STH reaction network in a single reactor entails syngas conversion to MeOH (Reaction R1), MeOH dehydration to DME (Reaction R2), and HC synthesis from DME (Reaction R3; represented with a balanced reaction for triptane synthesis with H_2 incorporation, as previously demonstrated using Cu/BEA[10]). This system also has the known side reaction of water-gas shift (WGS, Reaction R4), which can be catalyzed by metallic Cu in the CZA and Cu/BEA catalysts.[25,26] The WGS reaction is important in this system as it relates to carbon loss via the production of CO_2 from syngas, but conversely, potential carbon efficiency gains through the conversion of co-fed CO_2 via the reverse-WGS reaction to produce CO for subsequent conversion to HCs via Reactions R1−R3 (*vide infra*). When feeding syngas, Reactions R1, R2, and R3 occur sequentially in this scheme for STH, suggesting that an optimum HC yield can be achieved by controlling the relative performance of each catalyst and/or the mass ratio of catalysts in the reactor. However, thermodynamic equilibrium considerations at the reaction temperature studied here (220 °C) are necessary as they will limit the extent of each reaction.[29] Although all four reactions are exothermic under these conditions (ΔH° values from −23.0 to −813 kJ mol^{-1}) and Reaction R3 has a large equilibrium constant (K_{eq} of 10^{140}, eqs S1−S3) that renders HC formation from DME essentially irreversible, large equilibrium constants are not found in all cases. Notably, the first reaction in the sequence, MeOH synthesis, has a low K_{eq} value of 0.0081 at this temperature. Also, the presence of MeOH and water, which are essential to achieve subsequent HC production, have important implications on the reaction network. For example, the reverse of Reactions R1 and R2 can occur when large concentrations of MeOH and water are present, respectively, which is especially problematic because of the small equilibrium constant for Reaction R1 at the targeted conditions. Therefore, to overcome the low CO conversion dictated by the thermodynamic limitations of Reaction R1, the equilibrium CO conversion during STH can be increased in a single-reactor through a synergistic effect between Reactions R1 and R2. Specifically, including a MeOH dehydration catalyst serves to minimize the in situ MeOH concentration and increase the total flux of CO through Reaction R1 (i.e., into subsequent reactions) than would otherwise be achieved if Reaction R1 was performed independently. Similarly, the irreversible consumption of DME to HCs in Reaction R3 enables a greater net flux of MeOH through Reaction R2. The equilibrium constants are only a function of the temperature and not pressure for the four gas-phase reactions in the STH reaction network; however, by exploiting La Chatelier's principle, increased MeOH yield can be achieved by increasing the absolute reactor pressure (common practice for industrial MeOH synthesis). This thermodynamic analysis highlights the cooperative advantages of a single reactor for STH and outlines the research challenge to balance reaction rates and equilibria of each step to achieve an overall performance that would not be achieved if the reactions were performed independently.

$$CO + 2H_2 \rightleftarrows CH_3OH \quad (R1)$$

$$2CH_3OH \rightleftarrows CH_3OCH_3 + H_2O \quad (R2)$$

$$7CH_3OCH_3 + 2H_2 \rightarrow 2C_7H_{16} + 7H_2O \quad (R3)$$

$$CO + H_2O \rightleftarrows CO_2 + H_2 \quad (R4)$$

where Reaction R1: $\Delta H^\circ = -90.4$ kJ mol^{-1}; $K_{eq,rxn1}(T = 220\ ^\circ C) = 0.0081$; Reaction R2: $\Delta H^\circ = -23.0$ kJ mol^{-1}; $K_{eq,rxn2}(T = 220\ ^\circ C) = 24.4$; Reaction R3: $\Delta H^\circ = -813$ kJ mol^{-1};[30] $K_{eq,rxn3}(T = 220\ ^\circ C) \approx 10^{140}$; Reaction R4: $\Delta H^\circ = -41.0$ kJ mol^{-1}; $K_{eq,rxn4}(T = 220\ ^\circ C) = 157$.

3.2. STH Performance of H/BEA and Cu/BEA in Different Bed Configurations. As an initial assessment of the STH reaction network over our multicomponent catalyst system, syngas conversion was investigated with "mixed-bed" and "stacked-bed" catalyst configurations (Figure 2) combining three catalysts: MeOH synthesis catalyst ($CuZnO/Al_2O_3$, "CZA"), MeOH dehydration catalyst (γ-Al_2O_3 or "A"), and a

https://doi.org/10.1021/acscatal.2c02155
ACS Catal. 2022, 12, 9270−9280

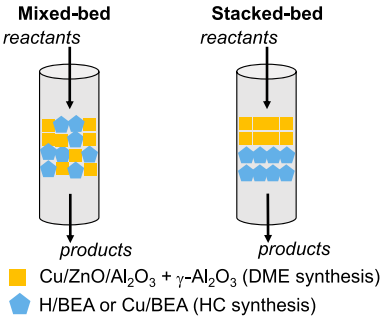

Figure 2. Schematic of mixed-bed and stacked-bed configurations for STH reactions employing H/BEA and Cu/BEA as the hydrocarbon (HC) synthesis catalyst.

H/BEA (SiO_2:Al_2O_3 = 27) or Cu/BEA (4.3 wt % Cu) HC synthesis catalyst.[10,11] The performance of Cu/BEA was compared to the parent H/BEA to investigate if the enhanced performance exhibited by Cu/BEA with a DME feed[10−12] also occurred with a syngas feed. The mixed-bed and stacked-bed configurations with catalyst mass ratio compositions of 3:1:1 for CZA:γ-Al_2O_3:H/BEA (or Cu/BEA) were compared at conditions of 220 °C, 750 kPa, and a H_2:CO mol ratio of 2:1, which is representative of that from biomass feedstocks after CO_2 removal.[24] An initial space velocity of 0.8 g_{CO} g_{CZA+A}^{-1} h^{-1} was employed for the first 6 h of reaction time to target an intermediate CO conversion (20−30%) during the typical induction period of the H/BEA and Cu/BEA catalysts.[10,11] The space velocity was then decreased to 0.3 g_{CO} g_{CZA+A}^{-1} h^{-1} for detailed analyses and comparisons between catalysts at greater CO conversions (>40%). In this initial set of experiments, all catalyst combinations demonstrated stable activity over the 18−22 h time period without evidence of substantial deactivation (Figure S1). The performance metrics compared here for the different catalyst combinations (Table 1 and Figure 3) are an average of the data collected from 9−16 h time on stream (TOS). As noted above, the C_{4+} products provide a versatile mixture to access HOG and SAF products, and therefore, we will focus on this product slate as a metric of performance.[11]

Table 1. Data from STH Reactions with Mixed-Bed and Stacked-Bed Catalyst Configurations of CZA:A:BEA Mass Ratio of 3:1:1[a]

	CZA:A:H/BEA		CZA:A:Cu/BEA	
	mixed	stacked	mixed	stacked
CO conversion (%)	47.1	53.0	42.5	52.8
DME yield (%)	12.2	36.1	3.1	16.1
C_{4+} yield (%)	12.9	3.1	16.3	13.0
Total hydrocarbon productivity ($g\ g_{BEA}^{-1}\ h^{-1}$)	0.093	0.024	0.120	0.093
CO_2 C-selectivity (%)	45.1	31.3	51.1	35.1

[a]Reaction conditions were 220 °C, 750 kPa, H_2:CO ratio of 2:1, and space velocity of 0.3 g_{CO} g_{CZA+A}^{-1} h^{-1}. Hydrocarbon productivity was normalized by mass of H/BEA or Cu/BEA. Reported values are an average of data over 9−16 h time on stream.

For H/BEA, the single-pass CO conversion was slightly lower in the mixed-bed configuration compared to the stacked-bed (Table 1, 47.1 vs 53.0%, respectively). The equilibrium-limited CO conversion for syngas to DME under these conditions is 47% (Section S2, for Reactions R1, R2, and R4).

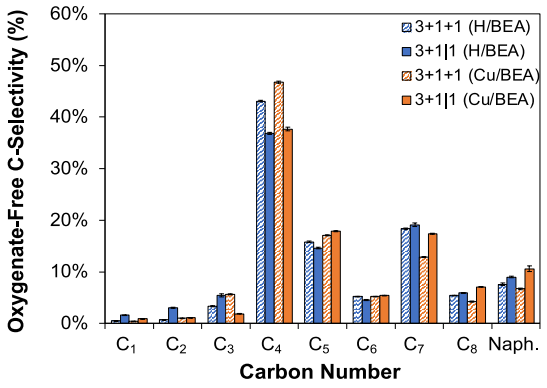

Figure 3. Oxygenate-free carbon selectivity for H/BEA (blue) and Cu/BEA (orange) in mixed-bed (dashed) and stacked-bed (solid) configurations with a CZA:A:BEA mass ratio of 3:1:1. Reaction conditions were 220 °C, 750 kPa, H_2:CO ratio of 2:1, and space velocity of 0.3 g_{CO} g_{CZA+A}^{-1} h^{-1}. Values are an average of data over 9−16 h time on stream, with error bars representing 99% confidence intervals. "Naph." indicates C_{9+} and cyclic C_{8+} hydrocarbons, as previously observed.[9]

The observation of CO conversion at or above the equilibrium-limited value confirms our hypothesis that the cascade chemistry of MeOH/DME synthesis followed by HC synthesis may enable a greater single-pass conversion of CO to HCs in a single reactor than would be permitted based on thermodynamics for single-pass CO to MeOH followed by HC synthesis in a subsequent reactor. In both configurations, the HC product oxygenate-free carbon selectivities were comparable to those observed with a DME feed,[10−12] displaying the characteristic low selectivity for C_{1-3} products and high selectivity for C_4 and C_7 products (Figure 3, Tables S2 and S3). The stacked-bed exhibited lower selectivity for C_4 (36.8 vs 43.1%) and slightly greater selectivity for C_7 (19.1 vs 18.4%) compared to the mixed-bed. A portion of C_{8+} products was also observed, and like C_7 selectivity, the stacked-bed exhibited greater selectivity to these higher carbon-number, fuel-range products. A benefit of the stacked-bed configuration was the substantially decreased CO_2 selectivity, which decreased from 45.1 to 31.3%. Carbon yields to C_{4+} products with H/BEA were 12.9% for the mixed-bed compared to just 3.1% for the stacked-bed. Unreacted DME intermediates were observed in both cases, with a greater yield (36.1 vs 12.2%) associated with the lower activity of the stacked-bed configuration. Thus, the lower HC yield observed from the stacked-bed was not due to insufficient DME production. We propose that the improved yield of C_{4+} HCs from the mixed-bed CZA+A+H/BEA configuration compared to stacked-bed CZA+A|H/BEA can be attributed to metallic Cu from CZA in close proximity to the H/BEA active sites, promoting H_2 activation and incorporation into the products during HC synthesis. This hypothesis is supported by results from our previous report for the conversion of DME to HCs with co-fed H_2, where improved HC yield was observed using a physical mixture of H/BEA and H_2-activating metallic Cu/SiO_2 compared to H/BEA alone.[10]

For Cu/BEA, greater CO conversion was also observed for the stacked-bed (Table 1, 52.8%) compared to the mixed-bed (42.5%), and both were near or above the equilibrium limitation for syngas to DME. Similar to the trends observed for H/BEA, the carbon selectivities to C_4 and C_{7+} were the most affected by the change from mixed-bed to stacked-bed

https://doi.org/10.1021/acscatal.2c02155
ACS Catal. 2022, 12, 9270−9280

(decrease of 9.2% for C_4 and increase of 4.5% for C_{7}, Figure 3), and substantially lower CO_2 selectivity was observed for the stacked-bed (35.1 vs 51.1%). Unreacted DME was also observed in both configurations, but nearly complete DME conversion (3.1% yield) was observed for the mixed-bed. Unlike H/BEA, comparable C_{4+} yields of 13.0 and 16.3% were observed for both configurations of Cu/BEA, which has metallic Cu near the zeolite active sites, adding further support to the assignment that Cu promotes HC synthesis in this STH reaction.

Considering the full data sets for H/BEA and Cu/BEA in both bed configurations, a few trends emerged that informed a down selection of catalyst composition and configuration for further investigation. The two mixed beds demonstrated comparably high CO conversions and C_{4+} yields, with correspondingly high values for total hydrocarbon productivity (i.e., gravimetric activity) of 0.093 and 0.120 g g_{BEA}^{-1} h^{-1} for H/BEA and Cu/BEA. However, both resulted in undesired high CO_2 selectivity (above 45%). These greater C_{4+} yields and HC production rates for the mixed-bed configurations may be attributed to the ability to better minimize in situ MeOH and DME concentrations through the catalyst bed, overcoming equilibrium limitations for the reaction network (Table S1). However, the unwanted high CO_2 selectivity may be attributed to the WGS reaction occurring on CZA in the lower portion of the mixed-bed catalyst, where unreacted CO is in contact with higher concentrations of water due to HC synthesis (Reaction R3) that occurs throughout the length of the mixed-bed configuration. In contrast, the stacked-bed configuration separates the WGS catalyst (CZA) from the water being produced during HC synthesis over Cu/BEA. The stacked-bed CO conversion for CZA+A|Cu/BEA (52.8%) was similar to that observed for CZA+A|H/BEA (53.0%), but the DME conversion was substantially greater for CZA+A|Cu/BEA, leading to disparate C_{4+} yields of 13.0 versus 3.1%, where the Cu/BEA catalyst clearly outperformed H/BEA in this configuration. This is reflected in the total HC productivity values, where the stacked CZA+A|Cu/BEA demonstrated a greater activity than CZA+A|H/BEA (0.093 versus 0.024 g g_{BEA}^{-1} h^{-1}). For both stacked-bed cases, the C_4 selectivity decreased with an associated increase in C_{7+} selectivity, and importantly, CO_2 selectivity decreased by ca. 14−16%. These selectivity data indicate that MeOH and DME synthesis occurring upstream from the (H or Cu)/BEA catalyst favors the hydrocarbon pool methylation chemistry, improving selectivity to C_{7+} products and simultaneously minimizing the WGS side-reaction in the second bed, resulting in decreased CO_2 selectivity. This effect is similar to a recent report utilizing CZA, γ-Al_2O_3, and a zeolite catalyst (ZSM-5, H-form, Si/Al = 97) in a single reactor, where improvements in HC selectivity and CO_2 selectivity were observed when CZA and γ-Al_2O_3 catalysts were upstream of the zeolite bed.[13,31] Based on the beneficial selectivity trends and the high performance of Cu/BEA in the stacked-bed configuration, CZA+A|Cu/BEA was chosen to further investigate the effects of process conditions on performance metrics, such as C_{4+} yield, and to explore CO_2 co-feeds.

3.3. Effect of Relative Catalyst Loading. Experiments were performed with increasing relative catalyst loading of Cu/BEA to explore the relationship between DME yield, HC yield, and carbon number selectivity toward achieving high single-pass C_{4+} yields. Systematic increases in the Cu/BEA catalyst mass, with constant CZA+A mass and constant total bed volume (by changing the mass of SiC diluent), provided a series of CZA+A|Cu/BEA compositions with mass ratios of 3+1|1, 3+1|2, and 3+1|3. Each composition was tested at the same reaction conditions from Section 3.2 (Table 2 and Figure 4). For these experiments, the data were compared at the same cumulative turnover number (TON = 80 ± 6 mol_C mol_{H+}^{-1}), because cumulative TON combines HC yield, reactant space velocity, and catalyst site density into a single term describing the hydrocarbon pool chemistry.[11,32] Comparing first the activity of these three compositions with increasing Cu/BEA content, the CO conversion only changed slightly from 52.2 to 56.2%, but the product yield of the DME intermediate decreased from 15.8 to 5.5%, indicating greater conversion of this oxygenate intermediate to the desired HC products. The corresponding C_{4+} yield increased from 15.8 to 19.1 to 23.5% with increasing Cu/BEA content. Despite the absolute decrease in the DME yield and related increase in the HC yield, a decrease in the gravimetric activity was observed with increasing Cu/BEA content (0.098 to 0.064 to 0.051 g $g_{Cu/BEA}^{-1}$ h^{-1}). This stepwise drop in productivity is attributed to the relationship between DME production and consumption in the STH cascade chemistry. The rate of DME

Table 2. Data from STH Reactions over Stacked-Bed CZA+A|Cu/BEA, with Increasing Amounts of Cu/BEA[a]

	CZA+A|Cu/BEA		
	3+1|1	3+1|2	3+1|3
CO conversion (%)	52.2	56.2	55.3
DME yield (%)	15.8	11.4	5.5
C_{4+} yield (%)	13.7	19.1	23.5
CO_2 C-selectivity (%)	35.2	39.0	39.0
C_{4+} C-selectivity (%)	28.3	37.3	47.1
Total hydrocarbon productivity (g $g_{Cu/BEA}^{-1}$ h^{-1})	0.098	0.064	0.051
Cumulative TON (mol_C mol_{H+}^{-1})	84	81	74

[a]Reaction conditions were 220 °C, 750 kPa, H_2:CO ratio of 2:1, and space velocity of 0.3 g_{CO} g_{CZA+A}^{-1} h^{-1}. TON data measured at ca. 10, 16, and 20 h TOS for bed ratios 3+1|1, 3+1|2, and 3+1|3, respectively.

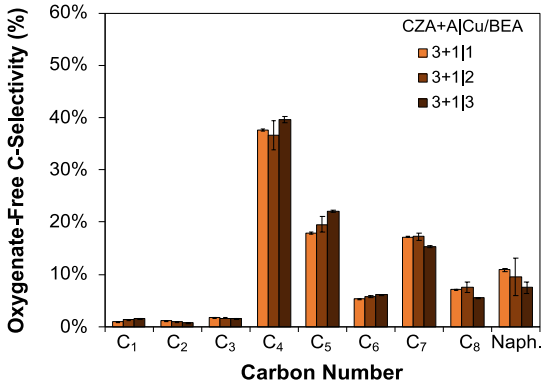

Figure 4. Oxygenate-free carbon selectivity for STH reactions over stacked-bed CZA+A|Cu/BEA, with increasing amounts of Cu/BEA from 3+1|1 to 3+1|3. Reaction conditions were 220 °C, 750 kPa, H_2:CO ratio of 2:1, and space velocity of 0.3 g_{CO} g_{CZA+A}^{-1} h^{-1}. Data reported at a cumulative TON of ca. 80 mol_C mol_{H+}^{-1} measured at ca. 10, 16, and 20 h TOS for bed ratios 3+1|1, 3+1|2, and 3+1|3, respectively, with error bars representing 99% confidence intervals.

https://doi.org/10.1021/acscatal.2c02155
ACS Catal. 2022, 12, 9270−9280

conversion to HCs is dependent on the rate of DME production, which is presumed to be constant across the three catalyst compositions because of the constant CZA+A mass in each composition. Thus, with greater relative Cu/BEA loading, there is an effective decrease in the concentration of DME per $g_{Cu/BEA}$, which in turn limits the HC formation rate throughout the Cu/BEA bed when normalized gravimetrically.

Comparing the selectivity of the three compositions, small changes in the CO_2 selectivity were observed with increasing Cu/BEA content (35.2−39.0%). Minor changes to the carbon number distributions were observed with increasing Cu/BEA content, where the selectivity to C_4 products increased from 37.6 to 39.5%, and inversely, the selectivity to C_7 decreased from 17.2 to 15.3% (Figure 4). This minor shift away from higher carbon number products with greater relative Cu/BEA content may be due to the decreasing concentration of DME available for methylation reactions or cracking of higher HCs at acid sites; another consequence of the concept presented above for the observed decrease in gravimetric activity. These data demonstrate that through control of the catalyst composition the conversion of syngas to HCs can be increased while maintaining high selectivity to C_{4+} products and decreasing the yield of the DME intermediate. It is also worth reiterating that compositions with greater relative Cu/BEA content did not lead to increased CO_2 selectivity via the WGS reaction.

Comparing the performance of our CZA+A|Cu/BEA catalyst system to those previously reported, one finds a wide range of CO conversions (20−90%) for the STH reaction through MeOH or DME intermediates. Therefore, here, we will focus on comparisons of product selectivity and yield. In reports of STO (syngas-to-olefins, 400 °C and 1−4 MPa) using oxide-zeolite catalysts (e.g., Zn-ZrO_2/SSZ-13), lower olefin products were targeted rather than fuel-range products, and high selectivities to C_{2-4} products (70−90%) were achieved with low C_{5+} selectivity (5−15%).[19,22,23] For STH reports targeting fuel-range products (C_{5-11}) with multicomponent catalyst systems (e.g., Cu/ZnO with ZSM-5) at intermediate temperature and high pressure (260−320 °C, 3.0 MPa), C_{5+} HC selectivities up to 84% were observed.[13,16,18] Under the more mild conditions of 220 °C and 750 kPa employed here, we observed a maximum C_{5+} HC selectivity of 58.5% using the 3+1|1 catalyst composition of CZA+A|Cu/BEA with an associated C_{1-3} selectivity of just 3.9%. This C_{5+} HC selectivity is largely dictated by the choice of zeolite, and Cu/BEA does not meet the highest selectivity reported in the literature using ZSM-5. However, the C_{5+} selectivity observed here is comparable to that typically reported from DME homologation over Cu/BEA zeolite (50−70%), and the product slate is aromatic-free.[9−12] Considering the C_{4+} products from Cu/BEA as a versatile mixture to access HOG and SAF products, as previously outlined,[11] a maximum C_{4+} HC selectivity of 96.1% was observed, highlighting the utility of the STH approach developed here to direct a high fraction of the carbon to renewable fuels.

Furthermore, minimizing CO_2 selectivity is key to developing an STH process with high carbon efficiency. The CO_2 selectivities reported for multicomponent oxide-zeolite catalyst systems ranged from 35−50%,[13,16,18] with the minimum value observed at 25% for a 0.5Pd/FeCuCo catalyst with ZSM-5 (300 °C and 7.0 MPa).[21] We observed CO_2 selectivities in a narrow range of 35−39% for CZA+A|Cu/BEA and demonstrated that controlling the catalyst composition affected the HC product yield but did not significantly affect CO_2 selectivity. The CZA+A|Cu/BEA catalyst achieved similar performance metrics at moderate temperature and pressure conditions (220 °C and 750 kPa, < 39% CO_2 selectivity, 96.1% C_{4+} selectivity within HC products) to a stacked-bed STH approach using CZA+A with a nano-ZSM-5 catalyst that employed much higher temperatures and pressures (300 °C and 3.0 MPa, 35% CO_2 selectivity, 85% C_{4+} selectivity).[13] In summary of these experiments exploring bed configuration and relative catalyst composition, a relatively low CO_2 selectivity was maintained with a high C_{4+} product distribution, leading to a single-pass C_{4+} yield as high as 23.5% (3+1|3, CZA+A|Cu/BEA), which is on the high end of the range of 13−28% previously reported for STH reactions.[13,16,17,21]

3.4. STH Performance Compared to DME Homologation. Previous reports from our group have focused on HOG and SAF production from biomass-derived DME at 200 °C and atmospheric pressure, highlighted by Cu/BEA exhibiting high selectivity to C_{4+} products with a greater HC formation rate than H/BEA.[9−12] In Table 3 and Figure 5, the results from

Table 3. Data from DME Conversion over Cu/BEA, and Syngas Conversion over Stacked-Bed CZA+A|Cu/BEA with Bed Ratios 3+1|1 and 3+1|3[a]

	Cu/BEA (DME)		CZA+A|Cu/BEA (STH)	
	200 °C	220 °C	3+1|1	3+1|3
DME or CO conversion (%)	9.1	17.6	52.2	55.3
C_{4+} yield (%)	6.4	13.2	13.7	23.5
total hydrocarbon productivity (g $g_{Cu/BEA}^{-1}$ h^{-1})	0.048	0.116	0.098	0.051
cumulative TON (mol_C mol_{H+}^{-1})	79	84	84	74

[a]For DME, the reaction conditions were 200 and 220 °C, 89 kPa, H_2:DME ratio of 1:1, and space velocity of 1.2 g_{DME} $g_{Cu/BEA}^{-1}$ h^{-1}. Data at 200 °C was previously reported in Wu et al.[12] For STH the reaction conditions were 220 °C, 750 kPa, H_2:CO ratio of 2:1, and space velocity of 0.3 g_{CO} g_{CZA+A}^{-1} h^{-1}. TON was measured at ca. 10 and 20 h for STH 3+1|1 and 3+1|3, respectively. DME TONs were measured at ca. 20 and 8 h for 200 and 220 °C, respectively.

STH experiments for two stacked-bed compositions, CZA+A|Cu/BEA of 3+1|1 and 3+1|3, are compared to performance data for Cu/BEA from DME conversion with co-fed H_2 at both 200 and 220 °C. Plots of DME conversion and C_{4+} yield versus time-on-stream during DME homologation at the two temperatures are provided in Figure S2. To account for the effects from the different reaction conditions (e.g., temperature, pressure, and space velocity) between the syngas and DME feeds, the data were compared at the same cumulative TON (80 ± 6 mol_C mol_{H+}^{-1}). For DME homologation under our typical conditions at 200 °C, markedly lower C_{4+} yield (6.4%) was observed compared to STH at 220 °C. Comparing DME homologation at 220 °C, STH reactions still resulted in greater yields of C_{4+} products for both CZA+A|Cu/BEA beds (13.7 and 23.5% for STH 3+1|1 and 3+1|3, respectively, compared to 13.2% for DME at 220 °C, Table 3). Notably, lower selectivity to C_7 products was observed from STH reactions for both bed compositions compared to DME feed (17.2 and 15.3% for 3+1|1 and 3+1|3, respectively, vs 19.5% for DME, Figure 5). Intermediate values for the gravimetric activity (normalized to $g_{Cu/BEA}$ as above) were observed during the STH reaction compared to DME homologation at both temperatures. The STH reaction exhibited a lower gravimetric

https://doi.org/10.1021/acscatal.2c02155
ACS Catal. 2022, 12, 9270−9280

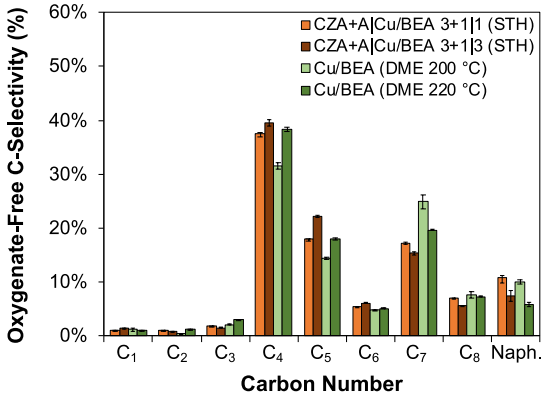

Figure 5. Oxygenate-free carbon selectivity for DME conversion over Cu/BEA, and STH over stacked-bed CZA+A|Cu/BEA with bed ratios 3+1|1 and 3+1|3. For DME, the reaction conditions were 200 or 220 °C, 89 kPa, H_2:DME ratio of 1:1, and space velocity of 1.2 g_{DME} $g_{Cu/BEA}^{-1}$ h^{-1}. Data at 200 °C were previously reported in Wu et al.[12] For STH, the reaction conditions were 220 °C, 750 kPa, H_2:CO ratio of 2:1, and space velocity of 0.3 g_{CO} g_{CZA+A}^{-1} h^{-1}. The data are reported at a common TON of 80 ± 6 mol_C mol_{H+}^{-1}. The TON values correspond to ca. 10 and 20 h TOS, for STH catalyst compositions of 3+1|1 and 3+1|3, respectively, and ca. 20 and 8 h for the DME homologation at 200 and 220 °C, respectively, with error bars representing 99% confidence intervals.

activity at the 3+1|1 and 3+1|3 bed compositions (0.098 and 0.051 g $g_{Cu/BEA}^{-1}$ h^{-1}, respectively) compared to the DME feed at the same temperature (0.116 g $g_{Cu/BEA}^{-1}$ h^{-1}), but greater activity than was previously reported at 200 °C (0.048 g $g_{Cu/BEA}^{-1}$ h^{-1}). Using Cu/BEA as the HC synthesis catalyst, these results highlight advantages of the STH reaction compared to DME homologation, where comparable or greater C_{4+} yield and gravimetric activity values were achieved during STH, while maintaining the desired selectivity toward C_{4+} HCs previously observed for DME homologation.

3.5. Co-Conversion of CO_2 with Syngas. Syngas from biomass or biogas typically contains appreciable amounts of CO_2, such as 19−23% of reformed biomass-derived syngas in a recent report.[24] In many instances, the CO_2 is removed prior to MeOH or fuel synthesis; however, a process able to co-convert CO_2 to produce high-value HC products would avoid the removal step and would conceptually improve the overall carbon efficiency. To explore the co-conversion of CO_2 in our STH approach, CO_2-rich and CO_2-free syngas conditions were studied (independent of previously described CO_2-free experiments, conducted without the 6 h induction period at higher space velocity, as described above). These experiments employed a 3+1|3 stacked-bed CZA+A|Cu/BEA configuration at a reaction temperature of 220 °C, pressure of 750 kPa, and with CO_2-rich or CO_2-free syngas (H_2:CO:CO_2 molar feed ratio of 2.5:1:0.9 or 2.5:1:0, corresponding to common compositions from biomass sources[24]). In experiments feeding CO and CO_2, conversion and yield treat both CO and CO_2 as reactants, according to eqs S10 and S11. The catalytic performance results are presented in Table 4. Without co-fed CO_2, the results were similar to those presented above, but exhibited moderately greater CO conversion (77.3%), C_{4+} yield (40.8%), and gravimetric activity (0.090 g $g_{Cu/BEA}^{-1}$ h^{-1}) with the higher H_2:CO ratio, along with no DME yield and comparable CO_2 selectivity (38.8%). With co-fed CO_2 at a 0.9:1.0 ratio of CO_2:CO, markedly lower conversion (19.5%) and C_{4+} yields (12.2%) were observed, which is not surprising

Table 4. Data from STH Reactions with and without Co-Fed CO_2[a]

	CZA+A|Cu/BEA: 3+1|3	
	without CO_2	with CO_2
CO or CO + CO_2 conversion (%)	77.3	56.1
DME yield (%)	0.0	0.0
C_{4+} yield (%)	44.9	12.2
CO_2 C-selectivity (%)	38.8	28.9
Total hydrocarbon productivity (g $g_{Cu/BEA}^{-1}$ h^{-1})	0.090	0.053

[a]Reaction conditions were 220 °C, 750 kPa, H_2:CO ratio of 2.5:1 or H_2:CO:CO_2 ratio of 2.5:1:0.9, and space velocity of 0.3 g_{CO} g_{CZA+A}^{-1} h^{-1}. Partial pressure of CO was 214 and 169 kPa, respectively.

considering the substantial decrease in CO partial pressure and replacement with the more difficult to activate CO_2 molecule. No DME product was detected, indicating full in situ consumption of DME. The gravimetric activity (0.053 g $g_{Cu/BEA}^{-1}$ h^{-1}) remained within the range previously observed for Cu/BEA (*vide supra*) but was approximately 40% lower than the CO_2-free value. Importantly, the HC selectivity was comparable to the CO_2-free experiments described throughout this report, exhibiting the characteristic distribution of low selectivity to C_{1-3} with high C_{4+} selectivity (Figure S3). As a first indication of CO_2 affecting the reaction network, either through activation via reverse-WGS or by suppressing CO_2 formation through equilibrium considerations, the CO_2 carbon selectivity with the CO_2-rich syngas feed decreased by 25% relative to the CO_2-free feed (28.9% compared to 38.8%). Finally, it is worth noting that this CO_2 selectivity of 28.9% was comparable to the lowest reported in previous STH chemistry (ca. 25%),[21] while maintaining moderate C_{4+} yield values (Table 3).

To investigate if CO_2 participated in the reaction network, and specifically, the HC synthesis reactions, isotopically labeled $^{13}CO_2$ experiments were performed. At constant reaction conditions of pressure, temperature, and H_2:CO:CO_2 ratio (750 kPa, 220 °C, and 2.5:1:0.9), either unlabeled or labeled CO_2 was fed to the stacked-bed CZA+A|Cu/BEA (3+1|3) catalyst, and ^{13}C in the HC products was monitored using mass spectrometry. In Figure 6, the mass spectra for abundant C_{4-7} HC species are compared between the $^{13}CO_2$ co-feed (red) and the unlabeled $^{12}CO_2$ co-feed (blue) conditions. For each of these products, mass fragment peaks shifted to (m/z) + 1 or greater when $^{13}CO_2$ was fed, indicating CO_2 activation and propagation through the reaction network into the HC products. As an example, the peak which corresponds to the propyl fragment in isobutane, isopentane, and isohexane shifted from m/z 43 for $^{12}CO_2$ co-feed to m/z 44 and 45 for $^{13}CO_2$ co-feed (Figure 6a−c). Similarly, the butyl fragment of triptane at m/z 57 for ^{12}C shifted to m/z 58, 59, and 60 in the spectrum with the isotopically labeled $^{13}CO_2$ co-feed, indicating 1−3 ^{13}C species were incorporated into the product (Figure 6d). This mass spectrometry analysis illustrates that CO_2 is activated under these conditions, presumably via the reverse water gas shift reaction, and importantly, that CO_2 is incorporated into the HC products.

4. CONCLUSIONS

By employing commercially available MeOH synthesis ($CuZnO/Al_2O_3$, CZA) and MeOH to DME catalysts (γ-Al_2O_3, A) with H/BEA and Cu/BEA catalysts, we explored a

https://doi.org/10.1021/acscatal.2c02155
ACS Catal. 2022, 12, 9270−9280

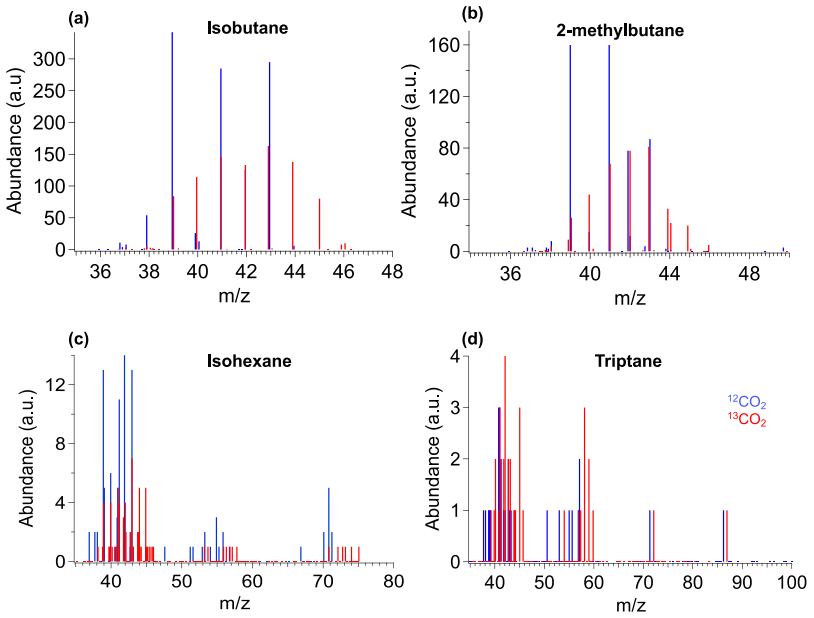

Figure 6. Mass spectra for four abundant hydrocarbon products during STH reactions with co-fed $^{12}CO_2$ or $^{13}CO_2$, (a) isobutane, (b) isopentane, (c) isohexane, and (d) triptane.

direct conversion route of syngas to hydrocarbons in a single reactor. Results using H/BEA and Cu/BEA demonstrate the importance of the proximity of Cu species to the BEA zeolite for the formation of C_4-and-C_7-rich HC product streams during the STH reactions, similar to our previous reports for the conversion of DME to HCs. Through a comparison of catalyst configurations, it was advantageous to position Cu/BEA in a stacked-bed configuration downstream of a CZA+A bed, which improved selectivity to C_{4+} HCs and favorably decreased CO_2 selectivity. Through control of the catalyst bed composition and process conditions, we demonstrated that the Cu/BEA activity in the STH reaction can meet or exceed that observed in the DME homologation reaction, with single-pass C_{4+} yields as high as 23.5% and gravimetric activity at the high-end of the range previously observed for Cu/BEA (up to 0.098 g $g_{Cu/BEA}^{-1}$ h^{-1} compared to 0.048−0.116 g $g_{Cu/BEA}^{-1}$ h^{-1} for DME homologation). Furthermore, with the CZA+AlCu/BEA stacked-bed configuration, we demonstrated that CO_2 can be co-converted with CO in a CO_2-rich syngas feed to generate HC products with similar selectivities to C_{4-7} products. Using a $^{13}CO_2$ co-feed and monitoring the products with mass spectrometry provided the critical evidence that carbon from co-fed CO_2 was incorporated into the HC products.

The results from this initial catalysis investigation of STH over the catalyst system reported here sets the foundation for applied engineering studies into the further development of this process intensification approach. First, utilizing one reactor for this STH pathway reduces the number of unit operations compared to the traditional three-step HOG pathway, with a corresponding opportunity to reduce the separation intensity necessary between units, serving to reduce overall capital and operating costs. The co-conversion of CO_2 reduces the requirement to remove CO_2 from syngas prior to HC synthesis and suggests that a full or partial CO_2 recycle may be feasible, which is expected to have economic benefits. Overall, these results, with continued development, provide an opportunity to increase carbon efficiency within the conceptual process to generate high-value, high-octane gasoline and sustainable aviation fuel.

■ ASSOCIATED CONTENT

Supporting Information

The Supporting Information is available free of charge at https://pubs.acs.org/doi/10.1021/acscatal.2c02155.

Equilibrium calculations (Section S1), STH time on stream data and hydrocarbon species identities (Section S2), DME to HOG time on stream data (Section S3), and CO_2 co-feed metric calculations and carbon selectivities (Section S4). The material is available free of charge (PDF)

■ AUTHOR INFORMATION

Corresponding Author

Daniel A. Ruddy − *Catalytic Carbon Transformation & Scale-Up Center, National Renewable Energy Laboratory, Golden, Colorado 80401, United States;* orcid.org/0000-0003-2654-3778; Email: dan.ruddy@nrel.gov

Authors

Claire T. Nimlos − *Catalytic Carbon Transformation & Scale-Up Center, National Renewable Energy Laboratory, Golden, Colorado 80401, United States*

Connor P. Nash − *Catalytic Carbon Transformation & Scale-Up Center, National Renewable Energy Laboratory, Golden, Colorado 80401, United States*

Daniel P. Dupuis − *Catalytic Carbon Transformation & Scale-Up Center, National Renewable Energy Laboratory, Golden, Colorado 80401, United States*

Anh T. To − *Catalytic Carbon Transformation & Scale-Up Center, National Renewable Energy Laboratory, Golden, Colorado 80401, United States;* orcid.org/0000-0002-1594-1730

Anurag Kumar − *Catalytic Carbon Transformation & Scale-Up Center, National Renewable Energy Laboratory, Golden, Colorado 80401, United States*

https://doi.org/10.1021/acscatal.2c02155
ACS Catal. 2022, 12, 9270−9280

Jesse E. Hensley − *Catalytic Carbon Transformation & Scale-Up Center, National Renewable Energy Laboratory, Golden, Colorado 80401, United States*

Complete contact information is available at: https://pubs.acs.org/10.1021/acscatal.2c02155

Author Contributions

The manuscript was written through contributions of all authors. All authors have given approval to the final version of the manuscript.

Notes

The authors declare no competing financial interest.

■ ACKNOWLEDGMENTS

This work was authored by the National Renewable Energy Laboratory, operated by Alliance for Sustainable Energy, LLC, under Contract No. DE-AC36-08GO28308. Funding was provided by the U.S. DOE Office of Energy Efficiency and Renewable Energy, Bioenergy Technologies Office in collaboration with the Chemical Catalysis for Bioenergy (ChemCatBio) Consortium, a member of the Energy Materials Network (EMN). The views expressed in this article do not necessarily represent the views of the DOE or the U.S. Government. The U.S. Government retains and the publisher, by accepting the article for publication, acknowledges that the U.S. Government retains a nonexclusive, paid-up, irrevocable, worldwide license to publish or reproduce the published form of this work, or allow others to do so, for U.S. Government purposes. The authors thank J. A. Schaidle (NREL) for helpful discussions of preliminary data.

■ REFERENCES

(1) Wood, D. A.; Nwaoha, C.; Towler, B. F. Gas-to-Liquids (GTL): A Review of an Industry Offering Several Routes for Monetizing Natural Gas. *J. Nat. Gas Sci. Eng.* **2012**, *9*, 196−208.

(2) Rauch, R.; Hrbek, J.; Hofbauer, H. Biomass Gasification for Synthesis Gas Production and Applications of the Syngas. *Wiley Interdiscip. Rev.: Energy Environ.* **2014**, *3*, 343−362.

(3) Tan, E. C. D.; Snowden-Swan, L. J.; Talmadge, M.; Dutta, A.; Jones, S.; Ramasamy, K. K.; Gray, M.; Dagle, R.; Padmaperuma, A.; Gerber, M.; Sahir, A. H.; Tao, L.; Zhang, Y. Comparative Techno-Economic Analysis and Process Design for Indirect Liquefaction Pathways to Distillate-Range Fuels via Biomass-Derived Oxygenated Intermediates Upgrading. *Biofuels, Bioprod. Biorefin.* **2017**, *11*, 41−66.

(4) *Final Rule for Control of Hazardous Air Pollutants from Mobile Sources*; Other Policies and Guidance EPA420-F-07-017; U.S. Environmental Protection Agency, Office of Transportation and Air Quality: Washington, DC, 2007; p 5.

(5) Tan, E. C.; Talmadge, M.; Dutta, A.; Hensley, J.; Snowden-Swan, L. J.; Humbird, D.; Schaidle, J.; Biddy, M. Conceptual Process Design and Economics for the Production of High-Octane Gasoline Blendstock via Indirect Liquefaction of Biomass through Methanol/Dimethyl Ether Intermediates. *Biofuels, Bioprod. Biorefin.* **2016**, *10*, 17−35.

(6) Ahn, J. H.; Temel, B.; Iglesia, E. Selective Homologation Routes to 2,2,3-Trimethylbutane on Solid Acids. *Angew. Chem., Int. Ed.* **2009**, *48*, 3814−3816.

(7) Simonetti, D. A.; Ahn, J. H.; Iglesia, E. Mechanistic Details of Acid-Catalyzed Reactions and Their Role in the Selective Synthesis of Triptane and Isobutane from Dimethyl Ether. *J. Catal.* **2011**, *277*, 173−195.

(8) Hazari, N.; Iglesia, E.; Labinger, J. A.; Simonetti, D. A. Selective Homogeneous and Heterogeneous Catalytic Conversion of Methanol/Dimethyl Ether to Triptane. *Acc. Chem. Res.* **2012**, *45*, 653−662.

(9) Nash, C. P.; Dupuis, D. P.; Kumar, A.; Farberow, C. A.; To, A. T.; Yang, C.; Wegener, E. C.; Miller, J. T.; Unocic, K. A.; Christensen, E.; Hensley, J. E.; Schaidle, J. A.; Habas, S. E.; Ruddy, D. A. Catalyst Design to Direct High-Octane Gasoline Fuel Properties for Improved Engine Efficiency. *Appl. Catal., B* **2022**, *301*, No. 120801.

(10) Schaidle, J. A.; Ruddy, D. A.; Habas, S. E.; Pan, M.; Zhang, G.; Miller, J. T.; Hensley, J. E. Conversion of Dimethyl Ether to 2,2,3-Trimethylbutane over a Cu/BEA Catalyst: Role of Cu Sites in Hydrogen Incorporation. *ACS Catal.* **2015**, *5*, 1794−1803.

(11) Ruddy, D. A.; Hensley, J. E.; Nash, C. P.; Tan, E. C. D.; Christensen, E.; Farberow, C. A.; Baddour, F. G.; Van Allsburg, K. M.; Schaidle, J. A. Methanol to High-Octane Gasoline within a Market-Responsive Biorefinery Concept Enabled by Catalysis. *Nat. Catal.* **2019**, *2*, 632−640.

(12) Wu, Q.; To, A. T.; Nash, C. P.; Dupuis, D. P.; Baddour, F. G.; Habas, S. E.; Ruddy, D. A. Spectroscopic Insight into Carbon Speciation and Removal on a Cu/BEA Catalyst during Renewable High-Octane Hydrocarbon Synthesis. *Appl. Catal., B* **2021**, *287*, No. 119925.

(13) Ni, Y.; Wang, K.; Zhu, W.; Liu, Z. Realizing High Conversion of Syngas to Gasoline-Range Liquid Hydrocarbons on a Dual-Bed-Mode Catalyst. *Chem Catal.* **2021**, *1*, 383−392.

(14) Chang, C. D.; Silvestri, A. J. The Conversion of Methanol and Other O-Compounds to Hydrocarbons over Zeolite Catalysts. *J. Catal.* **1977**, *47*, 249−259.

(15) Haw, J. F.; Song, W.; Marcus, D. M.; Nicholas, J. B. The Mechanism of Methanol to Hydrocarbon Catalysis. *Acc. Chem. Res.* **2003**, *36*, 317−326.

(16) Zhang, Q.; Li, X.; Asami, K.; Asaoka, S.; Fujimoto, K. Synthesis of LPG from Synthesis Gas. *Fuel Process. Technol.* **2004**, *85*, 1139−1150.

(17) Fujimoto, K.; Saima, H.; Tominaga, H. Synthesis Gas Conversion Utilizing Mixed Catalyst Composed of CO Reducing Catalyst and Solid Acid: IV. Selective Synthesis of C2, C3, and C4 Paraffins from Synthesis Gas. *J. Catal.* **1985**, *94*, 16−23.

(18) Li, N.; Jiao, F.; Pan, X.; Chen, Y.; Feng, J.; Li, G.; Bao, X. High-Quality Gasoline Directly from Syngas by Dual Metal Oxide−Zeolite (OX-ZEO) Catalysis. *Angew. Chem.* **2019**, *131*, 7478−7482.

(19) Jiao, F.; Li, J.; Pan, X.; Xiao, J.; Li, H.; Ma, H.; Wei, M.; Pan, Y.; Zhou, Z.; Li, M.; Miao, S.; Li, J.; Zhu, Y.; Xiao, D.; He, T.; Yang, J.; Qi, F.; Fu, Q.; Bao, X. Selective Conversion of Syngas to Light Olefins. *Science* **2016**, *351*, 1065−1068.

(20) Dagle, R. A.; Lizarazo-Adarme, J. A.; Lebarbier Dagle, V.; Gray, M. J.; White, J. F.; King, D. L.; Palo, D. R. Syngas Conversion to Gasoline-Range Hydrocarbons over $Pd/ZnO/Al_2O_3$ and ZSM-5 Composite Catalyst System. *Fuel Process. Technol.* **2014**, *123*, 65−74.

(21) Lebarbier Dagle, V. M.; Dagle, R. A.; Li, J.; Deshmane, C.; Taylor, C. E.; Bao, X.; Wang, Y. Direct Conversion of Syngas-to-Hydrocarbons over Higher Alcohols Synthesis Catalysts Mixed with HZSM-5. *Ind. Eng. Chem. Res.* **2014**, *53*, 13928−13934.

(22) Cheng, K.; Gu, B.; Liu, X.; Kang, J.; Zhang, Q.; Wang, Y. Direct and Highly Selective Conversion of Synthesis Gas into Lower Olefins: Design of a Bifunctional Catalyst Combining Methanol Synthesis and Carbon−Carbon Coupling. *Angew. Chem., Int. Ed.* **2016**, *55*, 4725−4728.

(23) Liu, X.; Zhou, W.; Yang, Y.; Cheng, K.; Kang, J.; Zhang, L.; Zhang, G.; Min, X.; Zhang, Q.; Wang, Y. Design of Efficient Bifunctional Catalysts for Direct Conversion of Syngas into Lower Olefins via Methanol/Dimethyl Ether Intermediates. *Chem. Sci.* **2018**, *9*, 4708−4718.

(24) Dupuis, D. P.; Grim, R. G.; Nelson, E.; Tan, E. C. D.; Ruddy, D. A.; Hernandez, S.; Westover, T.; Hensley, J. E.; Carpenter, D. High-Octane Gasoline from Biomass: Experimental, Economic, and Environmental Assessment. *Appl. Energy* **2019**, *241*, 25−33.

(25) Yahiro, H.; Murawaki, K.; Saiki, K.; Yamamoto, T.; Yamaura, H. Study on the Supported Cu-Based Catalysts for the Low-Temperature Water−Gas Shift Reaction. *Catal. Today* **2007**, *126*, 436−440.

(26) de Souza, T. R. O.; de Oliveira Brito, S. M.; Andrade, H. M. C. Zeolite Catalysts for the Water Gas Shift Reaction. *Appl. Catal., A* **1999**, *178*, 7−15.
(27) Muhler, M.; Törnqvist, E.; Nielsen, L. P.; Clausen, B. S.; Topsøe, H. On the Role of Adsorbed Atomic Oxygen and CO2 in Copper Based Methanol Synthesis Catalysts. *Catal. Lett.* **1994**, *25*, 1−10.
(28) Chinchen, G. C.; Spencer, M. S.; Waugh, K. C.; Whan, D. A. Promotion of Methanol Synthesis and the Water-Gas Shift Reactions by Adsorbed Oxygen on Supported Copper Catalysts. *J. Chem. Soc., Faraday Trans. 1* **1987**, *83*, 2193−2212.
(29) Moradi, G. R.; Ahmadpour, J.; Yaripour, F.; Wang, J. Equilibrium Calculations for Direct Synthesis of Dimethyl Ether from Syngas. *Can. J. Chem. Eng.* **2011**, *89*, 108−115.
(30) *CRC Handbook of Chemistry and Physics*, 85th ed.; Lide, D. R., Ed.; CRC Press: Boca Raton, FL, 2004.
(31) Lorenz, E.; Wehling, P.; Schlereth, M.; Kraushaar-Czarnetzki, B. Influence of the Spatial Arrangement of Catalyst Components in the Single-Stage Conversion of Synthesis Gas to Gasoline. *Catal. Today* **2016**, *275*, 183−190.
(32) Hwang, A.; Prieto-Centurion, D.; Bhan, A. Isotopic Tracer Studies of Methanol-to-Olefins Conversion over HSAPO-34: The Role of the Olefins-Based Catalytic Cycle. *J. Catal.* **2016**, *337*, 52−56.

https://doi.org/10.1021/acscatal.2c02155
ACS Catal. 2022, 12, 9270−9280